Published in final edited form as:
Gastroenterology. 2009 March ; 136(3): 1012–1024. doi:10.1053/j.gastro.2008.12.004.

EpCAM-positive hepatocellular carcinoma cells are tumor initiating cells with stem/progenitor cell features

Taro Yamashita[1], **Junfang Ji**[1], **Anuradha Budhu**[1], **Marshonna Forgues**[1], **Wen Yang**[2], **Hong-Yang Wang**[2], **Huliang Jia**[3], **Qinghai Ye**[3], **Lun-Xiu Qin**[3], **Elaine Wauthier**[4], **Lola M. Reid**[4], **Hiroshi Minato**[5], **Masao Honda**[5], **Shuichi Kaneko**[5], **Zhao-You Tang**[3], and **Xin Wei Wang**[1,a]

[1]Liver Carcinogenesis Section, Laboratory of Human Carcinogenesis, Center for Cancer Research, National Cancer Institute, Bethesda, MD 20892-4258, USA

[2]International Cooperation Laboratory on Signal Transduction, Eastern Hepatobiliary Surgery Institute, Shanghai 200438, China

[3]Liver Cancer Institute and Zhongshan Hospital, Fudan University, Shanghai 200032, China;

[4]Department of Cell and Molecular Physiology, University of North Carolina School of Medicine, Chapel Hill, NC 27599, USA

[5]Liver Disease Center and Kanazawa University Hospital, Kanazawa University, Kanazawa, 920-8641, Japan.

Abstract

Background & Aims—Cancer progression/metastases and embryonic development share many properties including cellular plasticity, dynamic cell motility, and integral interaction with the microenvironment. We hypothesized that the heterogeneous nature of hepatocellular carcinoma (HCC) may be, in part, due to the presence of hepatic cancer cells with stem/progenitor features.

Methods—Gene expression profiling and immunohistochemistry analyses were used to analyze 235 tumor specimens derived from two recently identified HCC subtypes ($EpCAM^+$ AFP^+ HCC and $EpCAM^-$ AFP^- HCC). These subtypes differed in their expression of alpha-fetoprotein (AFP), a molecule produced in the developing embryo, and EpCAM, a cell surface hepatic stem cell marker. Fluorescence-activated cell sorting (FACS) was used to isolate $EpCAM^+$ HCC cells, which were tested for hepatic stem/progenitor cell properties.

Results—Gene expression and pathway analyses revealed that the $EpCAM^+$ AFP^+ HCC subtype had features of hepatic stem/progenitor cells. Indeed, the FACS-isolated $EpCAM^+$ HCC cells displayed hepatic cancer stem cell-like traits including the abilities to self-renew and differentiate. Moreover, these cells were capable of initiating highly invasive HCC in NOD/SCID mice. Activation of Wnt/β-catenin signaling enriched the $EpCAM^+$ cell population, while RNA interference-based blockage of EpCAM, a Wnt/β-catenin signaling target, attenuated the activities of these cells.

Conclusions—Taken together, our results suggest that HCC growth and invasiveness is dictated by a subset of $EpCAM^+$ cells, opening a new avenue for HCC cancer cell eradication by targeting Wnt/β-catenin signaling components such as EpCAM.

aCorrespondence: Liver Carcinogenesis Section, LHC, CCR, NCI, 37 Convent Drive, Building 37, Room 3044A, MSC 4258, Bethesda, MD 20892-4258, USA; Phone: 301-496-2099; Fax: 301-496-0497; xw3u@nih.gov..

Disclosures: No conflicts of interest exist.

Microarray data: Publicly available at http://www.ncbi.nlm.nih.gov/geo/ (Accession number: GSE5975).

INTRODUCTION

Tumors originate from normal cells as a result of accumulated genetic/epigenetic changes. Although considered monoclonal in origin, tumor cells are heterogeneous in their morphology, clinical behavior, and molecular profiles [1, 2]. Tumor cell heterogeneity has previously been explained by the clonal evolution model [3], however, recent evidence has suggested that heterogeneity may be due to derivation from endogenous stem/progenitor cells [4] or de-differentiation of a transformed cell 5. This hypothesis supports an early proposal that cancers represent "blocked ontogeny" 6 and a derivative that cancers are transformed stem cells 7. This renaissance of stem cells as targets of malignant transformation has led to realizations about the similarities between cancer cells and normal stem cells in their capacity to self-renew, produce heterogeneous progenies, and limitlessly divide [8]. The cancer stem cell (CSC) (or Tumor Initiating Cell) concept is that a subset of cancer cells bears stem cell features that are indispensable for a tumor. Accumulating evidence suggests the involvement of CSCs in the perpetuation of various cancers including leukemia, breast cancer, brain cancer, prostate cancer and colon cancer [9-13]. Experimentally, putative CSCs have been isolated using cell surface markers specific for normal stem cells. Stem cell-like features of CSC have been confirmed by functional *in vitro* clonogenicity and *in vivo* tumorigenicity assays. For example, leukemia-initiating cells in NOD/SCID mice are $CD34^{++}CD38^{-}$ [11]. Breast cancer CSCs are $CD44^{+}CD24^{-/low}$ cells while tumor initiating cells of the brain, colon and prostate are $CD133^{+}$ [10, 12, 13]. CSCs are considered more metastatic and drug/radiation resistant than non-CSCs in the tumor, and are responsible for cancer relapse. These findings warrant the development of treatment strategies that can specifically eradicate CSCs [14, 15].

Hepatocellular carcinoma (HCC) is the third leading cause of cancer death worldwide [16]. Although the cellular origin of HCC is unclear 17, 18, HCC has heterogeneous pathologies and genetic/genomic profiles 19, suggesting that HCC can initiate in different cell lineages 20. The liver is considered as a maturational lineage system similar to that in the bone marrow [21]. Experimental evidence indicates that certain forms of hepatic stem cells (HpSC), present in human livers of all donor ages, are multipotent and can give rise to hepatoblasts (HB) 22, 23, which are, in turn, bipotent progenitor cells that can progress either into the hepatocytic or biliary lineages 22, 24. Alpha-fetoprotein (AFP) is one of the earliest markers detected in the liver bud specified from the ventral foregut [25, 26], but its expression has only been found in HB and to a lesser extent in committed hepatocytic progenitors, not in later lineages nor in normal human HpSC 22. Recent studies also indicate that EpCAM is a biomarker for HpSC as it is expressed in HpSCs and HBs [22-24].

We recently identified a novel HCC classification system based on EpCAM and AFP status [27]. Gene expression profiles revealed that $EpCAM^{+}$ AFP^{+} HCC (referred to as Hepatic Stem Cell-like HCC; HpSC-HCC) has progenitor features with poor prognosis, whereas $EpCAM^{-}$ AFP^{-} HCC (referred to as Mature Hepatocyte-like HCC; MH-HCC) have adult hepatocyte features with good prognosis. Wnt/β-catenin signaling, a critical player for maintaining embryonic stem cells [28], is activated in $EpCAM^{+}$ AFP^{+} HCC, and EpCAM is a direct transcriptional target of Wnt/β-catenin signaling [29]. Moreover, $EpCAM^{+}$ AFP^{+} HCC cells are more sensitive to β-catenin inhibitors than $EpCAM^{-}$ HCC cells *in vitro* [29]. Interestingly, a heterogeneous expression of EpCAM and AFP was observed in clinical tissues, a feature that may be attributed to the presence of a subset of CSCs. In this study, we have confirmed that $EpCAM^{+}$ HCC cells are highly invasive and tumorigenic, and have activated Wnt/β-catenin signaling. We also demonstrate a crucial role of EpCAM in the maintenance of hepatic CSCs. Our data shed new light on the pathogenesis of HCC and may open new avenues for therapeutic interventions for targeting hepatic CSCs.

Materials and Methods

Clinical Specimens

HCC samples were obtained with informed consent from patients who underwent radical resection at the Liver Cancer Institute of Fudan University, Eastern Hepatobiliary Surgery Institute and the Liver Disease Center of Kanazawa University Hospital, and the study was approved by the Institutional Review Board of the respective Institutes. The microarray data from clinical specimens are publicly available (GEO accession number, GSE5975) [27]. Array data from a total of 156 HCC cases (155 hepatitis B virus-positive) corresponding to two subtypes of HCC, i.e., HpSC-HCC and MH-HCC, were used to search for HpSC-HCC-associated genes (Suppl Table 3). A total of 79 formalin fixed and paraffin-embedded HCC samples were used for IHC analyses (Suppl Table 4), 56 of which were also used in a recent study [30]. The classification of HpSC-HCC and MH-HCC were based on previously described criteria [27].

Cell Cultures and Sorting

Human liver cancer cell lines (HuH1 and HuH7) were derived from Health Science Research Resources Bank (JCRB0199 and JCRB0403, respectively) and routinely cultured as previously described 31. Normal human MHs, provided by the University of Pittsburgh through LTPADS, were cultured as previously described 32. Human HpSCs were isolated from fetal livers and cultured in Kubota's Medium as previously described 33. Wnt10B conditioned medium was prepared as described 34. Embryonic stem cell culture medium was prepared using Knockout™ DMEM supplemented with 18% of Serum Replacement (Invitrogen). The pTOP-FLASH and pFOP-FLASH luciferase constructs were previously described [29]. BIO and MeBIO were generous gifts from Ali Brivanlou (The Rockefeller University, New York, NY). For isolating single cell-derived colonies to determine whether heterogeneity is an intrinsic property of $EpCAM^+$ cells, HuH1 and HuH7 cells were resuspended and plated as a single cell per well in 96-well plates. A total of 192 single cells were successfully plated. The clones which grew well were selected two weeks after seeding and used for IF analysis. The 5FU stock (2 mg/ml; Sigma, St. Louis, MO), was prepared in distilled water. Fluorescence Activated Cell Sorting (FACS) and Magnetic Activated Cell Sorting (MACS) analyses were used to isolate $EpCAM^+$ HCC cells (supplemental materials).

Clonogenicity, spheroid formation, invasion, quantitative RT-PCR and immunohistochemistry (IHC) assays

For colony formation assays, 2,000 $EpCAM^+$ or $EpCAM^-$ cells were seeded in 6-well plates after FACS. After 10 days of culture, cells were fixed by 100% methanol and stained with methylene blue. For spheroid assays, single cell suspensions of 1,000 $EpCAM^+$ or $EpCAM^-$ cells were seeded in 6-well Ultra-Low Attachment Microplates (Corning, Corning, NY) after FACS. The number of spheroids was measured 14 days after seeding. Invasion assays were performed using BD BioCoat™ Matrigel Matrix Cell Culture Inserts and Control Inserts (BD Biosciences) essentially as previously described [31]. RT-PCR and IHC assays are described in details in the supplemental materials.

Tumorigenicity in NOD/SCID Mice

Six-week-old NOD/SCID mice (NOD/NCrCRl-*Prkdc*^{scid}) were purchased from Charles River (Charles River Laboratories, Inc., Wilmington, MA). The protocol was approved by the NCI-Bethesda Animal Care and Use Committee. Cells were suspended in 200 μl of DMEM and Matrigel (1:1), and subcutaneous injection was performed. The size and incidence of subcutaneous tumors were recorded. For histological evaluation, tumors were formalin-fixed

paraffin-embedded or directly embedded in O.C.T. compound (Sakura Finetek, Torrance, CA) and stored in −80°C.

RNA interference

A siRNA specific to *TACSTD1* (SI03019667) and a control siRNA (1022076) were designed and synthesized by Qiagen (Qiagen, Valencia, CA). Transfection was performed using Lipofectamine 2000 (Invitrogen), according to the manufacturer's instructions. A total of 200 nM of siRNA duplex was used for each transfection.

Statistical Analyses

The class comparison and gene clustering analyses were performed as previously described [30]. The canonical pathway analysis was performed using Ingenuity Pathways Analysis (v5.5, Ingenuity® Systems). The association of HCC subtypes and clinicopathological characteristics was examined using either Mann-Whitney U-tests or χ^2 tests. Student t-tests were used to compare various test groups assayed by colony formation, spheroid formation or invasion assays. The Kaplan-Meier survival analysis was performed to compare patient survival or tumorigenecity.

RESULTS

A poor prognostic HCC subtype with molecular features of HpSC

We re-evaluated the gene expression profiles that were uniquely associated with two recently identified prognostic subtypes of HCC, i.e., HpSC-HCC and MH-HCC, using a publicly available microarray dataset of 156 HCC cases (GEO accession number: GSE5975). Sixty cases were defined as HpSC-HCC with a poor prognosis while 96 cases were defined as MH-HCC with a good prognosis, based on EpCAM and AFP status [27]. A class comparison analysis with univariate t-tests and a global permutation test (x1000) yielded 793 genes that were differentially expressed between HpSC-HCC and MH-HCC ($P < 0.001$). Hierarchical cluster analyses revealed two main gene clusters that were upregulated (cluster-A; 455 genes) or downregulated (cluster-B; 338 genes) in HpSC-HCC (Fig 1A). Pathway analysis indicated that the enriched genes in cluster-A were significantly associated with known stem cell signaling pathways such as TGF-β, Wnt/β-catenin, PI3K/Akt and integrin ($P < 0.01$) (Fig 1B). In contrast, genes in cluster-B were significantly associated with mature hepatocyte functions such as xenobiotic metabolism, complement system, and coagulation system ($P < 0.01$). Noticeably, known HpSC markers such as *KRT19* (CK19), *TACSTD1* (EpCAM), *AFP, DKK1, DLK1* and *PROM1* (CD133) were significantly upregulated in HpSC-HCC while known liver maturation markers such as *UGT2B7* and *CYP3A4* were more abundantly expressed in MH-HCC (Fig 1C) (Suppl Tables 1-2). Kaplan-Meier survival analysis revealed that HpSC-HCC patients had a significantly shorter survival than MH-HCC patients ($P = 0.036$) (Fig 1D). Consistently, HpSC-HCC patients had a high frequency of macroscopic and microscopic portal vein invasion (Fig 1E).

However, IHC analyses of an additional 79 HCC cases revealed that among 24 HpSC-HCC cases, EpCAM staining was very heterogeneous with a mixture of $EpCAM^+$ and $EpCAM^-$ tumor cells in each tumor (Fig 1F, **left panel**). Noticeably, many of the $EpCAM^+$ tumor cells were located at the invasion border zones and were often disseminated at the invasive front (black arrows). Immunofluorescence (IF) analysis revealed that HCC cells located at the invasive front co-expressed EpCAM, CK19, and AFP (Fig 1F, **right panels**). Noticeably, HpSC-HCC patients were significantly younger than MH-HCC patients (Suppl Tables 3-4). Enrichment of $EpCAM^+$ AFP^+ tumor cells at the tumor invasive front suggested their involvement in HCC invasion and metastasis.

Isolation and characterization of EpCAM$^+$ cells in HCC

The results above suggest that HpSC-HCC may be organized in a hierarchical fashion in which EpCAM$^+$ tumor cells act as stem-like cells with an ability to differentiate into EpCAM$^-$ tumor cells. To test this hypothesis, we first evaluated the expression pattern of seven hepatic stem/maturation markers (EpCAM, CD133, CD90, CK19, Vimentin, Hep-Par1, and β-catenin) in six HCC cell lines (Fig 2A). All three AFP$^+$ cell lines (HuH1, HuH7, and Hep3B) expressed EpCAM, CD133, and cytoplasmic/nuclear β-catenin, whereas the other three AFP$^-$ cell lines (SK-Hep-1, HLE, and HLF) did not, consistent with the microarray data. Interestingly, AFP$^+$ cell lines had no CD90$^+$ cell population which was recently identified as hepatic CSCs [35], whereas AFP$^-$ cell lines had such a population. Consistently with the IF data, FACS analysis showed that AFP$^+$ cell lines had a subpopulation of EpCAM$^+$ and CD133$^+$ but no CD90$^+$ cells, whereas AFP$^-$ cell lines had a subpopulation of CD90$^+$ cells but no EpCAM$^+$ nor CD133$^+$ cells (Fig 2B). These data indicate that HpSC-HCC and MH-HCC cell lines have distinct stem cell marker expression patterns, and EpCAM as well as CD133 may be hepatic CSC markers specifically in HpSC-HCC.

We selected two human HCC cell lines (HuH1 and HuH7) to isolate EpCAM+ cells since both lines were heterogeneous in EpCAM, AFP, CK19 and β-catenin expression (Fig 2A-B and Suppl Fig 1A) [29]. We successfully enriched EpCAM$^+$ and EpCAM$^-$ populations from HuH7 cells by fluorescence activated cell sorting (FACS), with >80% purity in EpCAM$^+$ cells and >90% in EpCAM$^-$ cells one day after sorting (Fig 3A). Similar results were obtained when the purity check was done immediately post-sorting (data not shown). EpCAM$^+$ cells were also positive for CK19 and β-catenin (Fig 3B and Suppl Fig 1B) and most were AFP$^+$ (data not shown). In contrast, EpCAM$^-$ cells were negative for these markers but positive for HepPar1, a monoclonal antibody specific to hepatocytes (Fig 3B). Consistent with the microarray data described above, the levels of *TACSTD1, MYC* and *hTERT* (known HpSC markers) were significantly increased in EpCAM$^+$ HuH7 cells, while the levels of *UGT2B7* and *CYP3A4* (known mature hepatocyte markers) were significantly higher in EpCAM$^-$ HuH7 cells (Fig 3C, **left upper panel**). This expression pattern was reminiscent of human HpSC cells (Fig 3C, **left lower panel**). Similar results were obtained from HuH1 cells (data not shown). We also compared gene expression patterns of isolated HuH1, HuH7, MH and HpSC cells using the TaqMan® Human Stem Cell Pluripotency Array containing 96 selected human stem cell-related genes. Although a differential expression pattern of stem cell related genes was evident among HpSC, EpCAM$^+$ HuH1 and EpCAM$^+$ HuH7 cells, EpCAM$^+$ HCC cells were more closely related to HpSC cells while EpCAM$^-$ HCC cells were more closely related to diploid adult mature hepatocytes (Fig 3C **right panel**, Suppl Fig 1C). Thus, it appeared that EpCAM$^+$ HCC cells had a gene expression pattern that is more closely related to HpSC than EpCAM$^-$ HCC cells.

The isolated EpCAM$^+$ HuH7 cells formed colonies efficiently while EpCAM$^-$ cells failed to do so (Fig 3D **upper and middle panel, and** Suppl Fig 2A **for HuH1 cells**). In addition, EpCAM$^+$ HuH7 cells were much more invasive than EpCAM$^-$ cells ($P < 0.03$) (Fig 3D **lower panel and** Suppl Fig 2B **for HuH1 cells**). The EpCAM$^+$ fraction decreased with time in sorted EpCAM$^+$ HuH7 cells from >80% to 50% (Fig 3E). However, a small percent of EpCAM$^+$ cells remained constant in sorted EpCAM$^-$ HuH7 cells. FACS analysis confirmed the results of IF analysis (Fig 3F and Suppl Fig 2C **for HuH7 and HuH1 cells, respectively**), suggesting that EpCAM$^+$ cells could differentiate into EpCAM$^-$ cells, eventually allowing an enriched EpCAM$^+$ fraction to revert back to parental cells after 14 days of culture. In contrast, EpCAM$^-$ cells maintained their EpCAM$^-$ status. In addition, we successfully isolated 12 HuH1 and 2 HuH7 colonies from 192 single cell-plated culture wells. However, all colonies were heterogeneous in EpCAM and AFP expression and no colony was completely EpCAM$^-$ (data not shown). Taken together, these results indicate that EpCAM$^+$ HCC cells resemble HpSC

features. It appears that EpCAM$^+$ cells, but not EpCAM$^-$ cells, have self-renewal and differentiation capabilities with the ability to form colonies from a single cell, and produce both EpCAM$^+$ and EpCAM$^-$ cells.

It has been previously demonstrated that stem/progenitor cells and cancer stem/progenitor cells can form spheroids *in vitro* in a non-attached condition [36, 37]. Consistently, EpCAM$^+$ cells could form spheroids efficiently, reaching to about 150~200 μm in diameter after 14 days culture (Fig 4A-B). Interestingly, all cells in a spheroid were EpCAM$^+$ while AFP expression was relatively heterogeneous (Fig 4C-D, Suppl Movie 1). Rarely, a few spheroids derived from an EpCAM$^-$ cell fraction were positive for EpCAM (data not shown), suggesting that these spheroids were derived from contaminated residual EpCAM$^+$ cells by FACS sorting. All spheroid cells maintained EpCAM expression while half of the attached cells lost EpCAM expression when the EpCAM$^+$ fraction was cultured for 14 days (Fig 4E). Most spheroid cells also abundantly expressed PCNA, implying active cell proliferation (Fig 4F and Suppl Movie 2). Thus, a subset of EpCAM$^+$ cells, but not EpCAM$^-$ cells, can form spheroids.

EpCAM$^+$ HCC cells as tumor initiating cells

EpCAM$^+$ HCC cells, but not EpCAM$^-$ HCC cells, could efficiently initiate invasive tumors in NOD/SCID mice (Fig 5). For example, 10,000 EpCAM$^+$ HuH1 cells produced large hypervascular tumors in 100% of mice whereas EpCAM$^-$ cell fractions produced only small and pale looking tumors in 30% of mice 4 weeks after injection (Fig 5A, Suppl Fig 3A). Similar results were obtained with HuH7 cells (Suppl Fig 3B-D). As little as 200 EpCAM$^+$ cells could initiate tumors in 8 of 10 injected mice, whereas 200 EpCAM$^-$ cells produced only one tumor among 10 injected mice at 6 weeks after transplantation, and the tumor sizes were much larger in the EpCAM$^+$ cells than the EpCAM$^-$ cells (Fig 5B and Suppl Fig 3E). EpCAM$^+$ cells produced tumors with a mixture of both EpCAM$^+$ and EpCAM$^-$ cells in xenografts, and these cells invaded in the capsule and muscles of the leg adjacent to the tumor (Fig 5C). EpCAM$^+$ cells derived from tumors again maintained their tumor initiating capacity, tumor morphology and invasive ability in an *in vivo* serial transplantation experiment (Fig 5D). Occasionally, EpCAM$^-$ cell fraction produced a few small tumors that always contain a mixture of EpCAM$^+$ and EpCAM$^-$ cells (data not shown), indicating that the tumor-initiating ability is contributed by the contaminated EpCAM$^+$ cells from FACS sorting.

To further validate whether EpCAM$^+$ HCC cells were tumor initiating cells, we isolated EpCAM$^+$ HCC cells from two cases of AFP$^+$ (>600 ng/ml serum AFP) HCC clinical specimens using MACS. Consistently, 1×10^4 EpCAM$^+$ cells could induce tumors in NOD/SCID mice, but up to 1×10^6 EpCAM$^-$ cells failed to do so (Table 1). In addition, similar to HCC cell lines, fresh EpCAM$^+$ tumor cells from two clinical HCC specimens were more efficient in forming spheroids *in vitro* than EpCAM$^-$ cells (Suppl Fig 4).

FACS analysis results indicate that a majority of EpCAM$^+$ cells express CD133 in HuH7 cells but not in HuH1 cells (Fig 2B), which prompted us to compare the tumorigenic capacity of EpCAM$^+$ and CD133$^+$ cells in these cell lines. Noticeably, EpCAM$^+$ HuH1 cells showed marked tumor initiating capacity compared with CD133$^+$ HuH1 cells (Fig 5E-F), whereas EpCAM$^+$ and CD133$^+$ cells had the similar tumorigenic ability in HuH7 cells (data not shown).

GSK-3β inhibition augments EpCAM$^+$ HCC cells

To determine the role of Wnt/β-catenin signaling [28] in EpCAM$^+$ HCC cells (Fig 1B), we first treated HuH1, HuH7, and HLF cells with a GSK-3β inhibitor BIO (Fig 6A), which activates Wnt/β-catenin signaling (Fig 6B) and maintains undifferentiation of embryonic stem cells [38]. BIO increased the EpCAM$^+$ cell population in HuH1 and HuH7 cells when compared to the control methylated BIO (MeBIO) (Fig 6A). In contrast, BIO had no effect on the CD90$^+$ cell

population that is more tumorigenic than the CD90$^-$ cell population in HLF (Fig 6A and data not shown). Enrichment of EpCAM$^+$ cells was further provoked by the treatment of Wnt10B-conditioned media in HuH7 cells (Fig 6C) [34]. BIO induced morphological alteration of HuH7 cells as most cells became small and round when compared to MeBIO and suppressed EpCAM$^-$ AFP$^-$ cell population (Fig 6D). Moreover, BIO induced *TACSTD1, MYC*, and *hTERT* expression and spheroid formation (Fig 6E-F).

EpCAM blockage by RNA interference

One of the hallmarks of CSCs is its resistance to conventional chemotherapeutic agents resulting in tumor relapse and thus targeting CSCs is critical to achieve successful tumor remission. Consistently, 5-FU could increase the EpCAM$^+$ population and spheroid formation of HuH1 and HuH7 cells (Fig 7A-B) (data not shown), suggesting a differential sensitivity of EpCAM$^+$ and EpCAM$^-$ HCC cells to 5-FU. In contrast, EpCAM blockage via RNA interference dramatically decreased the population of EpCAM$^+$ cells (Fig 7C), and significantly inhibited cellular invasion, spheroid formation and tumorigenicity of HuH1 cells (Fig 7D-F). Thus, EpCAM may serve as a molecular target to eliminate HCC cells with stem/progenitor cell features.

DISCUSSION

The cellular origin of HCC is currently in debate. In this study, we found that EpCAM can serve as a marker to enrich HCC cells with tumor initiating ability and with some stem/progenitor cell traits. EpCAM is expressed in many human cancers with an epithelium origin 39. During embryogenesis, EpCAM is expressed in fertilized oocytes, embryonic stem cells and embryoid bodies, suggesting its role in early stage embryogenesis 40. Furthermore, a recent paper indicates that EpCAM is expressed in colonic and breast CSCs 41. Taken together, these data suggest a critical role of EpCAM in CSCs as well as embryonic and somatic stem cells. Consistently, we found that EpCAM expression is regulated by Wnt/β-catenin signaling [29] and tumorigenic and highly invasive HpSC-HCC is orchestrated by a subset of cells expressing EpCAM and AFP with stem cell-like features and self-renewal and differentiation capabilities regulated by Wnt/β-catenin signaling (this study). Thus, EpCAM may be a common gene expressed in undifferentiated normal and HCC with activated Wnt/β-catenin signaling. It may act as a downstream molecule to maintain HCC "stemness" and serve as a good marker for HCC initiating cells.

CD133 or CD90 have been used to identify potential hepatic CSCs [35, 42]. CD133 is expressed in normal and malignant stem cells of the neural, hematopoietic, epithelial, hepatic and endothelial lineages [23, 43, 44], suggesting that CD133 is also a common marker to detect normal and CSCs. Captivatingly, EpCAM expression overlaps with CD133 expression in normal human colon tissues and colorectal cancer tissues, yet CD133$^+$ and CD133$^-$ cells are equally tumorigenic 45. Similarly, we found that EpCAM$^+$ and EpCAM$^-$ HuH1 cells equally expressed CD133 but only EpCAM$^+$ cells developed large hypervascular tumors. Our data suggest that EpCAM may be a better marker than CD133 to enrich HCC tumor initiating cells from AFP$^+$ tumors. We also found that CD90 expression was limited to HCC cell lines that are EpCAM$^-$ AFP$^-$, and Wnt/β-catenin signaling had little effect on CD90$^+$ cell enrichment. These results suggest that the expression patterns of various stem cell markers in tumor initiating cells with stem/progenitor cell features may be different in each HCC subtype, possibly due to the heterogeneity of activated signaling pathways in normal stem/progenitor cells where these tumor initiating cells may originate. Therefore, it would be useful to comprehensively investigate the expression patterns of stem cell markers to characterize the population of CSC that may correlate with the activation of their distinct molecular pathways.

CSCs may be more resistant to chemotherapeutic agents than differentiated tumor cells possibly due to an increased expression of ATP-binding cassette transporters and anti-apoptotic proteins [4]. Thus, development of an effective strategy to target CSC pools together with conventional chemotherapies is essential to eradicate a tumor mass [14]. By blocking the programs that activate self-renewal and/or inhibit asymmetric division, CSC features could be "destemmed" [46, 47]. Consistently, EpCAM blockage could inhibit cellular invasion and tumorigenicity of $EpCAM^+$ HCC cells, revealing the feasibility of targeting a CSC marker to "destem" CSC features. EpCAM may induce c-Myc [48], a common molecular node activated in HpSC-HCC [27]. c-Myc, together with Oct3/4, Sox2, and Klf4, can induce pluripotent stem cells from adult fibroblasts [49]. It is possible that EpCAM blockage to inhibit hepatic CSCs may result in a suppression of c-Myc signaling. Encouragingly, EpCAM-specific antibodies are currently in phase II clinical trials [50].

Furthermore, a recent study indicates that $EpCAM^+$ circulating tumor cells identified by a unique microfluidic platform can be used to monitor patient outcomes undergoing systemic treatment [51]. Therefore, it may be useful to combine EpCAM antibodies with conventional chemotherapy to target both CSCs and non-CSCs for the treatment of HCC.

Supplementary Material

Refer to Web version on PubMed Central for supplementary material.

Acknowledgments

We thank Drs. Curtis Harris and Sharon Pine for critical readings of the manuscript; Ms. Barbara Taylor and Dr. Susan Garfield for technical assistance; Drs. Ali Brivanlou (Rockefeller University), Steve Strom (University of Pittsburgh), and Bert Vogelstein (Johns Hopkins University) for generously providing their research materials.

Grant Support: This work was supported in part by the Intramural Research Program of the Center for Cancer Research, the US National Cancer Institute. H.-L.J, Q.-H.Y., L.-X.Q, and Z.-Y.T. were supported by the research grants from the China National Natural Science Foundation for Distinguished Young Scholars (30325041) and the China National "863" R&D High-Tech Key Project (2002BA711A02-4). L.M.R. was supported by a sponsored research grant from Vesta Therapeutics (Research Triangle Park, NC), NIH grants (RO1 AA014243 , RO1 IP30-DK065933), and a U.S. Department of Energy grant (DE-FG02-02ER-63477). Sponsors have no role in the study design, data collection, analysis and interpretation.

References

1. Fialkow PJ. Clonal origin of human tumors. Biochim Biophys Acta 1976;458:283–321. [PubMed: 1067873]
2. Heppner GH. Tumor heterogeneity. Cancer Res 1984;44:2259–2265. [PubMed: 6372991]
3. Hanahan D, Weinberg RA. The hallmarks of cancer. Cell 2000;100:57–70. [PubMed: 10647931]
4. Jordan CT, Guzman ML, Noble M. Cancer stem cells. N Engl J Med 2006;355:1253–1261. [PubMed: 16990388]
5. Clarke MF, Dick JE, Dirks PB, et al. Cancer stem cells--perspectives on current status and future directions: AACR Workshop on cancer stem cells. Cancer Res 2006;66:9339–9344. [PubMed: 16990346]
6. Potter VR. Phenotypic diversity in experimental hepatomas: the concept of partially blocked ontogeny. The 10th Walter Hubert Lecture. Br J Cancer 1978;38:1–23. [PubMed: 356869]
7. Sell S. Cellular origin of cancer: dedifferentiation or stem cell maturation arrest? Environ Health Perspect 1993;101(Suppl 5):15–26. [PubMed: 7516873]
8. Wicha MS, Liu S, Dontu G. Cancer stem cells: an old idea--a paradigm shift. Cancer Res 2006;66:1883–1890. [PubMed: 16488983]
9. Al Hajj M, Wicha MS, Benito-Hernandez A, et al. Prospective identification of tumorigenic breast cancer cells. Proc Natl Acad Sci U S A 2003;100:3983–3988. [PubMed: 12629218]

10. Singh SK, Hawkins C, Clarke ID, et al. Identification of human brain tumour initiating cells. Nature 2004;432:396–401. [PubMed: 15549107]
11. Bonnet D, Dick JE. Human acute myeloid leukemia is organized as a hierarchy that originates from a primitive hematopoietic cell. Nat Med 1997;3:730–737. [PubMed: 9212098]
12. Ricci-Vitiani L, Lombardi DG, Pilozzi E, et al. Identification and expansion of human colon-cancer-initiating cells. Nature 2007;445:111–115. [PubMed: 17122771]
13. O'Brien CA, Pollett A, Gallinger S, et al. A human colon cancer cell capable of initiating tumour growth in immunodeficient mice. Nature 2007;445:106–110. [PubMed: 17122772]
14. Dean M, Fojo T, Bates S. Tumour stem cells and drug resistance. Nat Rev Cancer 2005;5:275–284. [PubMed: 15803154]
15. Rich JN. Cancer stem cells in radiation resistance. Cancer Res 2007;67:8980–8984. [PubMed: 17908997]
16. Parkin DM, Bray F, Ferlay J, et al. Global cancer statistics, 2002. CA Cancer J Clin 2005;55:74–108. [PubMed: 15761078]
17. Sell S, Pierce GB. Maturation arrest of stem cell differentiation is a common pathway for the cellular origin of teratocarcinomas and epithelial cancers. Lab Invest 1994;70:6–22. [PubMed: 8302019]
18. Thorgeirsson SS, Grisham JW. Hepatic stem cells. Semin Liver Dis 2003;23:301.
19. Thorgeirsson SS, Grisham JW. Molecular pathogenesis of human hepatocellular carcinoma. Nat Genet 2002;31:339–346. [PubMed: 12149612]
20. Lee JS, Heo J, Libbrecht L, et al. A novel prognostic subtype of human hepatocellular carcinoma derived from hepatic progenitor cells. Nat Med 2006;12:410–416. [PubMed: 16532004]
21. Sigal SH, Brill S, Fiorino AS, et al. The liver as a stem cell and lineage system. Am J Physiol 1992;263:G139–G148. [PubMed: 1325126]
22. Schmelzer E, Wauthier E, Reid LM. The Phenotypes of Pluripotent Human Hepatic Progenitors. Stem Cells 2006;24:1852–1858. [PubMed: 16627685]
23. Schmelzer E, Zhang L, Bruce A, et al. Human hepatic stem cells from fetal and postnatal donors. J Exp Med 2007;204:1973–1987. [PubMed: 17664288]
24. Dan YY, Riehle KJ, Lazaro C, et al. Isolation of multipotent progenitor cells from human fetal liver capable of differentiating into liver and mesenchymal lineages. Proc Natl Acad Sci U S A 2006;103:9912–9917. [PubMed: 16782807]
25. Zaret KS. Regulatory phases of early liver development: paradigms of organogenesis. Nat Rev Genet 2002;3:499–512. [PubMed: 12094228]
26. Shafritz DA, Oertel M, Menthena A, et al. Liver stem cells and prospects for liver reconstitution by transplanted cells. Hepatology 2006;43:S89–S98. [PubMed: 16447292]
27. Yamashita T, Forgues M, Wang W, et al. EpCAM and alpha-fetoprotein expression defines novel prognostic subtypes of hepatocellular carcinoma. Cancer Res 2008;68:1451–1461. [PubMed: 18316609]
28. Reya T, Clevers H. Wnt signalling in stem cells and cancer. Nature 2005;434:843–850. [PubMed: 15829953]
29. Yamashita T, Budhu A, Forgues M, et al. Activation of hepatic stem cell marker EpCAM by Wnt-ß-catenin signaling in hepatocellular carcinoma. Cancer Research 2007;67:10831–10839. [PubMed: 18006828]
30. Budhu A, Forgues M, Ye QH, et al. Prediction of venous metastases, recurrence and prognosis in hepatocellular carcinoma based on a unique immune response signature of the liver microenvironment. Cancer Cell 2006;10:99–111. [PubMed: 16904609]
31. Ye QH, Qin LX, Forgues M, et al. Predicting hepatitis B virus-positive metastatic hepatocellular carcinomas using gene expression profiling and supervised machine learning. Nat Med 2003;9:416–423. [PubMed: 12640447]
32. Wu CG, Forgues M, Siddique S, et al. SAGE transcript profiles of normal primary human hepatocytes expressing oncogenic hepatitis B virus X protein. FASEB J 2002;16:1665–1667. [PubMed: 12207007]

33. Kubota H, Reid LM. Clonogenic hepatoblasts, common precursors for hepatocytic and biliary lineages, are lacking classical major histocompatibility complex class I antigen. Proc Natl Acad Sci U S A 2000;97:12132–12137. [PubMed: 11050242]
34. Yoshikawa H, Matsubara K, Zhou X, et al. WNT10B Functional Dualism: beta-Catenin/Tcf-dependent Growth Promotion or Independent Suppression with Deregulated Expression in Cancer. Mol Biol Cell 2007;18:4292–4303. [PubMed: 17761539]
35. Yang ZF, Ho DW, Ng MN, et al. Significance of CD90(+) Cancer Stem Cells in Human Liver Cancer. Cancer Cell 2008;13:153–166. [PubMed: 18242515]
36. Dontu G, Abdallah WM, Foley JM, et al. In vitro propagation and transcriptional profiling of human mammary stem/progenitor cells. Genes Dev 2003;17:1253–1270. [PubMed: 12756227]
37. Fang D, Nguyen TK, Leishear K, et al. A tumorigenic subpopulation with stem cell properties in melanomas. Cancer Res 2005;65:9328–9337. [PubMed: 16230395]
38. Sato N, Meijer L, Skaltsounis L, et al. Maintenance of pluripotency in human and mouse embryonic stem cells through activation of Wnt signaling by a pharmacological GSK-3-specific inhibitor. Nat Med 2004;10:55–63. [PubMed: 14702635]
39. Balzar M, Winter MJ, de Boer CJ, et al. The biology of the 17-1A antigen (Ep-CAM). J Mol Med 1999;77:699–712. [PubMed: 10606205]
40. Trzpis M, McLaughlin PM, de Leij LM, et al. Epithelial cell adhesion molecule: more than a carcinoma marker and adhesion molecule. Am J Pathol 2007;171:386–395. [PubMed: 17600130]
41. Dalerba P, Dylla SJ, Park IK, et al. Phenotypic characterization of human colorectal cancer stem cells. Proc Natl Acad Sci U S A 2007;104:10158–10163. [PubMed: 17548814]
42. Ma S, Chan KW, Hu L, et al. Identification and characterization of tumorigenic liver cancer stem/progenitor cells. Gastroenterology 2007;132:2542–2556. [PubMed: 17570225]
43. Yin AH, Miraglia S, Zanjani ED, et al. AC133, a novel marker for human hematopoietic stem and progenitor cells. Blood 1997;90:5002–5012. [PubMed: 9389720]
44. Fargeas CA, Corbeil D, Huttner WB. AC133 antigen, CD133, prominin-1, prominin-2, etc.: prominin family gene products in need of a rational nomenclature. Stem Cells 2003;21:506–508. [PubMed: 12832703]
45. Shmelkov SV, Butler JM, Hooper AT, et al. CD133 expression is not restricted to stem cells, and both CD133+ and CD133− metastatic colon cancer cells initiate tumors. J Clin Invest 2008;118:2111–2120. [PubMed: 18497886]
46. Hill RP, Perris R. "Destemming" cancer stem cells. J Natl Cancer Inst 2007;99:1435–1440. [PubMed: 17895479]
47. Piccirillo SG, Reynolds BA, Zanetti N, et al. Bone morphogenetic proteins inhibit the tumorigenic potential of human brain tumour-initiating cells. Nature 2006;444:761–765. [PubMed: 17151667]
48. Munz M, Kieu C, Mack B, et al. The carcinoma-associated antigen EpCAM upregulates c-myc and induces cell proliferation. Oncogene 2004;23:5748–5758. [PubMed: 15195135]
49. Takahashi K, Tanabe K, Ohnuki M, et al. Induction of pluripotent stem cells from adult human fibroblasts by defined factors. Cell 2007;131:861–872. [PubMed: 18035408]
50. Chaudry MA, Sales K, Ruf P, et al. EpCAM an immunotherapeutic target for gastrointestinal malignancy: current experience and future challenges. Br J Cancer 2007;96:1013–1019. [PubMed: 17325709]
51. Nagrath S, Sequist LV, Maheswaran S, et al. Isolation of rare circulating tumour cells in cancer patients by microchip technology. Nature 2007;450:1235–1241. [PubMed: 18097410]

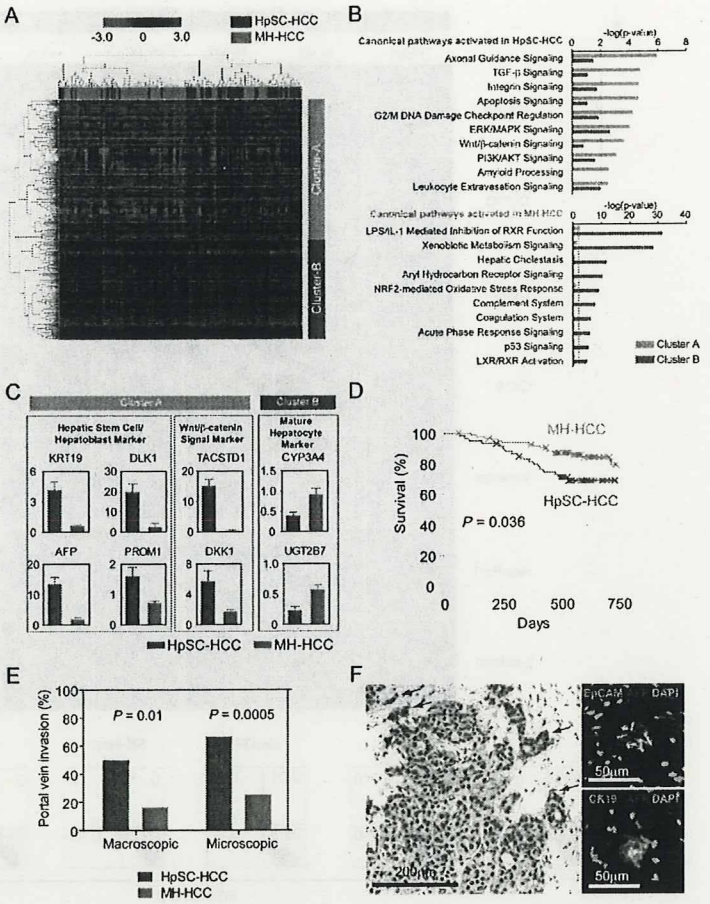

Figure 1.

HpSC-HCC represents a subset of invasive HCCs with cancer stem cells (CSC) Features. (A) Hierarchical cluster analysis based on 793 HpSC-HCC-coregulated genes in 156 HCC cases. Each cell in the matrix represents the expression level of a gene in an individual sample. Red and green cells depict high and low expression levels, respectively, as indicated by the scale bar. (B) Pathway analysis of HpSC-HCC-coregulated genes. The top ten canonical signaling pathways activated in cluster-A (upper panel) or cluster-B (lower panel) with statistical significance ($P < 0.01$) are shown. (C) Expression patterns of well-known HpSC and MH markers in each HCC subtype as analyzed by microarray. (D) Kaplan-Meier survival analysis of the cases used for array analysis. (E) Frequency of macroscopic and microscopic portal vein invasion in HpSC-HCC and MH-HCC used for IHC. (F) Representative images of EpCAM, AFP, and CK19 staining in HpSC-HCC samples analyzed by IHC and IF. EpCAM staining illustrates heterogeneous expression of EpCAM in HpSC-HCC (left panel). $EpCAM^+$ cells were disseminated in the invasive border (left panel black arrows) with expression of AFP (right top panel) and CK19 (right bottom panel).

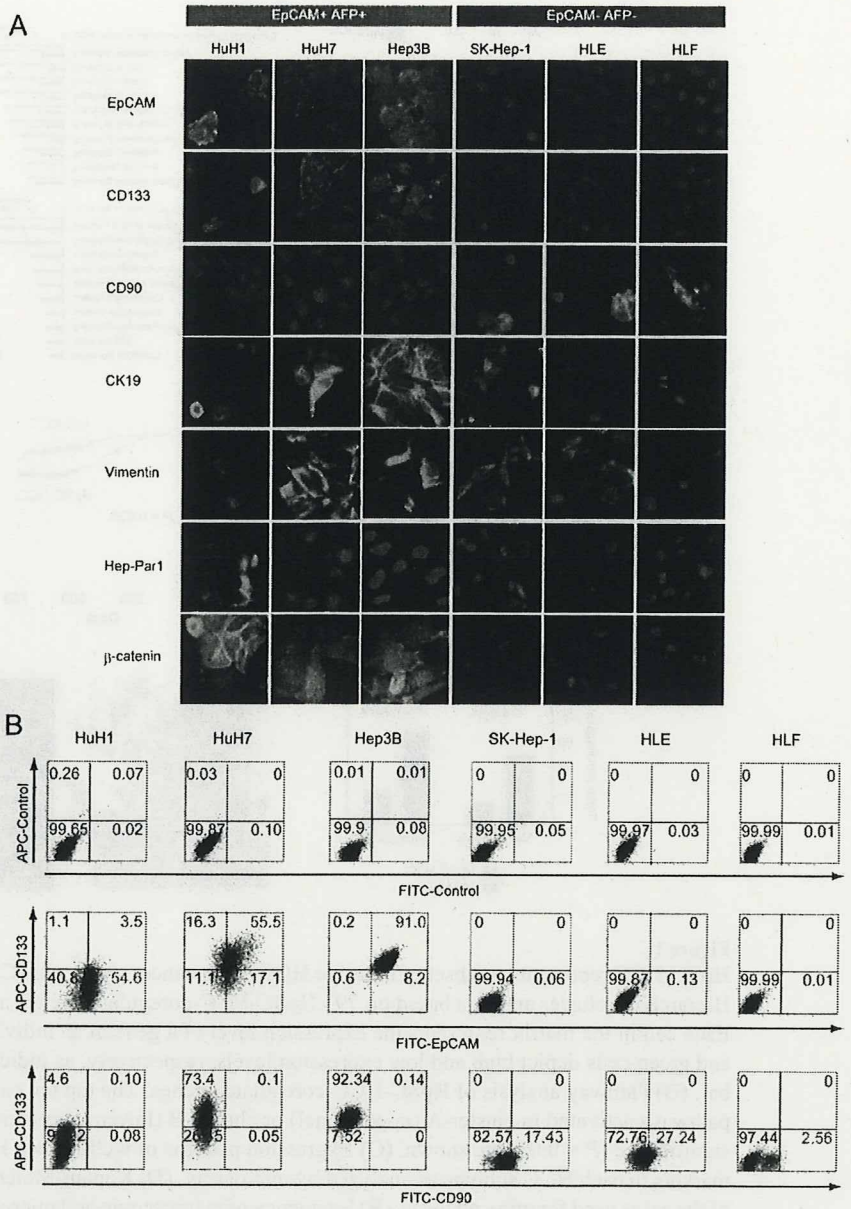

Figure 2.

Characterization of hepatic stem cell marker expression in HCC cell lines. (A) IF analysis of six HCC cell lines ($EpCAM^+$ AFP^+ cell lines; HuH1, HuH7, and Hep3B, $EpCAM^-$ AFP^- cell lines; SK-Hep-1, HLE, and HLF) stained with anti-EpCAM, anti-CD133, anti-CD90, anti-CK19, anti-Vimentin, anti-Hep-Par1, and anti-β-catenin antibodies. (B) FACS analysis of six HCC cell lines stained with anti-EpCAM, anti-CD133, and anti-CD90 antibodies.

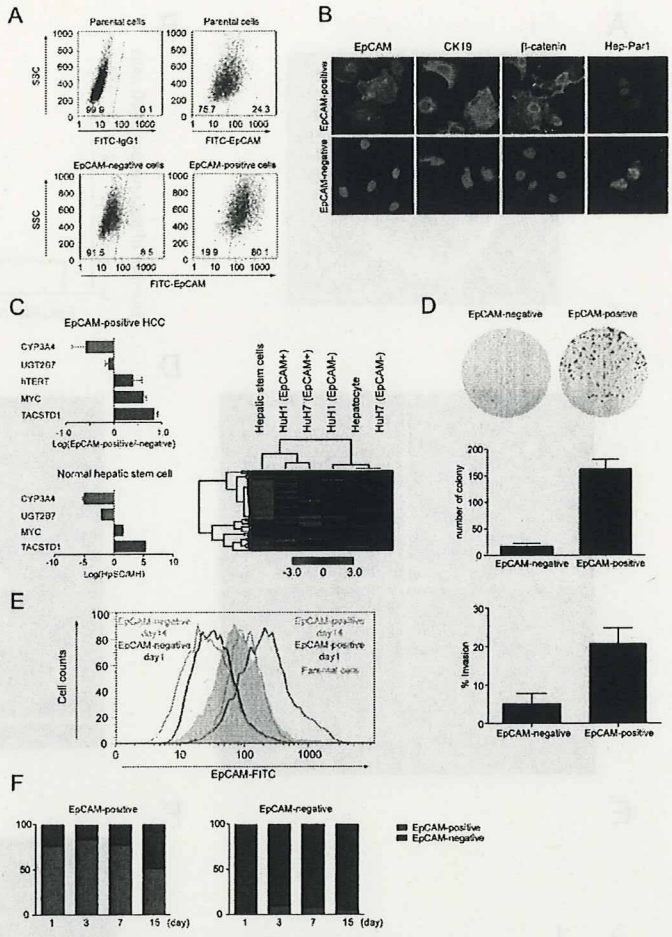

Figure 3.

Characterization of EpCAM$^+$ and EpCAM$^-$ cells in HuH7 cells. (A) FACS analysis of EpCAM$^+$ and EpCAM$^-$ cells day 1 after cell sorting. (B) IF analysis of cells stained with anti-EpCAM, anti-AFP, anti-CK19, or anti-β-catenin antibodies. (C) qRT-PCR analysis of EpCAM$^+$ and EpCAM$^-$ HuH7 cells (left upper panel) or hepatic stem cells (HpSC) and mature hepatocytes (MH) (left lower panel). Experiments were performed in triplicate. Hierarchical cluster analysis of HpSC, MH, EpCAM$^+$ and EpCAM$^-$ HCC cells using a panel of genes expressed in human embryonic stem cells (right panel). Gene expression was measured in quadruplicate. (D) Representative photographs of the plates containing colonies derived from 2,000 EpCAM$^+$ or EpCAM$^-$ HuH7 cells (upper panel). Colony formation experiments were performed in triplicate (mean ± SD) (middle panel). Cell invasiveness of EpCAM$^+$ and EpCAM$^-$ cells using the Matrigel invasion assay (lower panel). (E) Flow cytometer analysis of EpCAM$^+$ and EpCAM$^-$ HuH7 cells stained with anti-EpCAM at day 1 and 14 after cell sorting. (F) Percent of sorted EpCAM$^+$ and EpCAM$^-$ cells after culturing with various times as analyzed by IF. Numbers of EpCAM$^+$ and EpCAM$^-$ cells were counted in three independent areas of Chamber Slides at day 1, 3, 7, and 15 after cell sorting. The average percentages of EpCAM$^+$ or $^-$ cells are depicted as red or blue, respectively.

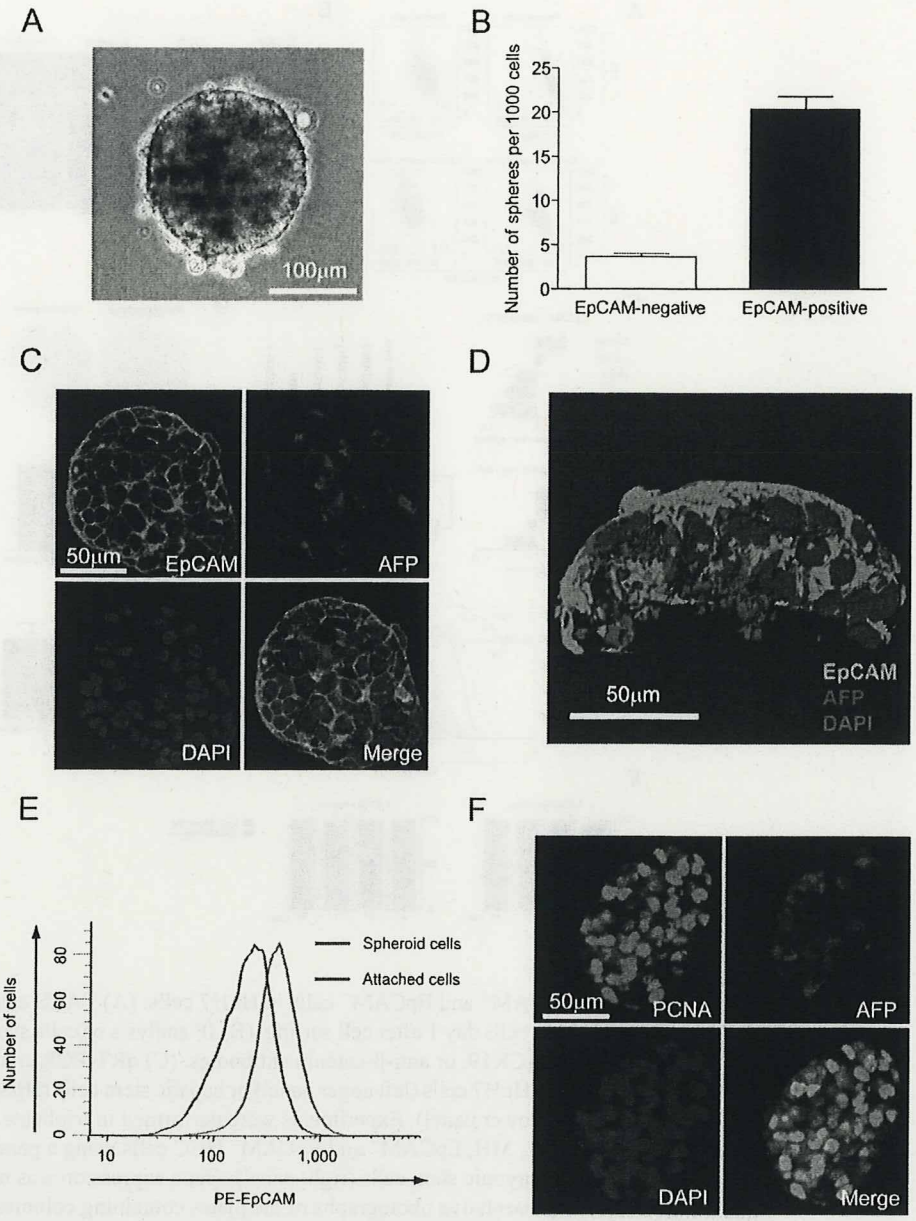

Figure 4.

Spheroid formation of EpCAM$^+$ HuH1 HCC cells. A representative phase contrast image of an HCC spheroid derived from an EpCAM$^+$ cell (scale bar = 100 μm) (A) and total numbers of spheroids from 1,000 sorted cells (B) are shown. Experiments were performed in triplicate and data are shown as mean ± SD. (C) Representative confocal images of an HCC spheroid co-stained with anti-EpCAM, anti-AFP and DAPI (scale bar = 50 μm). (D) A 3-D image of an HCC spheroid co-stained with anti-EpCAM, anti-AFP and DAPI (scale bar = 50 μm) reconstructed from confocal images using surface rendering. (E) FACS analysis of EpCAM$^+$ cells cultured as spheroids cells (red) or attached cells (blue) for 14 days after cell sorting. (F)

Confocal images of an HCC spheroid co-stained with anti-PCNA, anti-AFP and DAPI (scale bar = 50 μm).

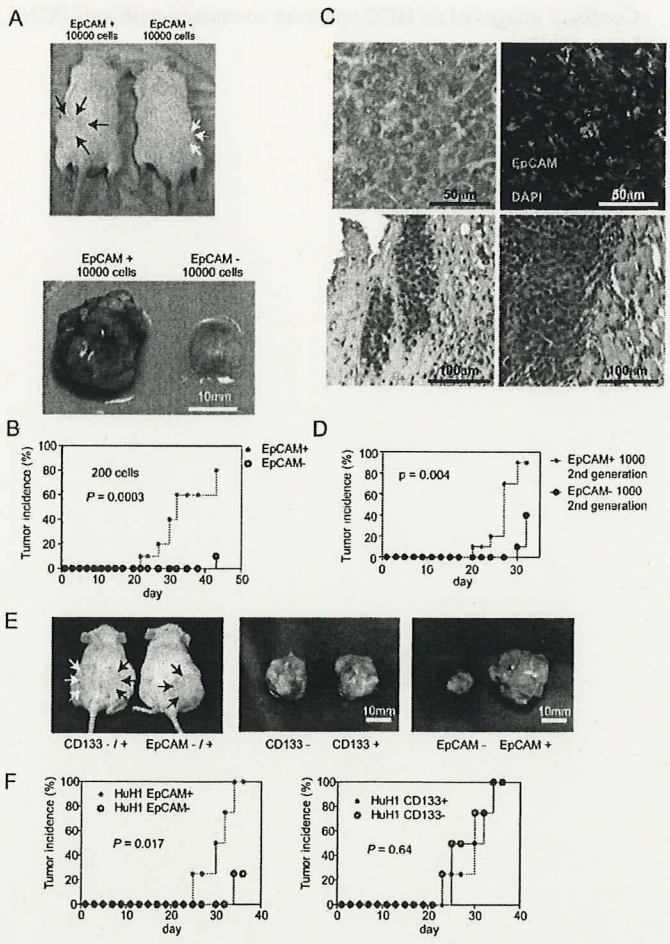

Figure 5.

Tumorigenic and invasive potential of EpCAM$^+$ HCC cells. (A) Representative NOD/SCID mice (upper panel) with subcutaneous tumors (lower panel) from EpCAM$^+$ (black arrows) or EpCAM$^-$ (white arrows) HuH1 cells. (B) Tumorigenicity of 200 sorted HuH1 cells. (C) Histological analysis of EpCAM$^+$ HuH1-derived xenografts. H&E staining of a subcutaneous tumor (left upper panel) with capsular invasion (left lower panel) and muscular invasion (right lower panel) and IF of the tumor stained with anti-EpCAM, anti-AFP, and DAPI (right upper panel) (scale bar = 50 μm). (D) Tumorigenicity of 1,000 sorted cells derived from an EpCAM$^+$ HuH1 xenograft. Data are generated from 10 mice in each group. (E) Representative NOD/SCID mice (left panel) with subcutaneous tumors from CD133$^+$ (black arrows) or CD133$^-$ (white arrows) (mid panel) and EpCAM$^+$ (black arrows) or EpCAM$^-$ (white arrows) (right panel) HuH1 cells. (F) Tumorigenicity of 1,000 HuH1 cells sorted by anti-EpCAM (left panel) or anti-CD133 (right panel) antibodies.

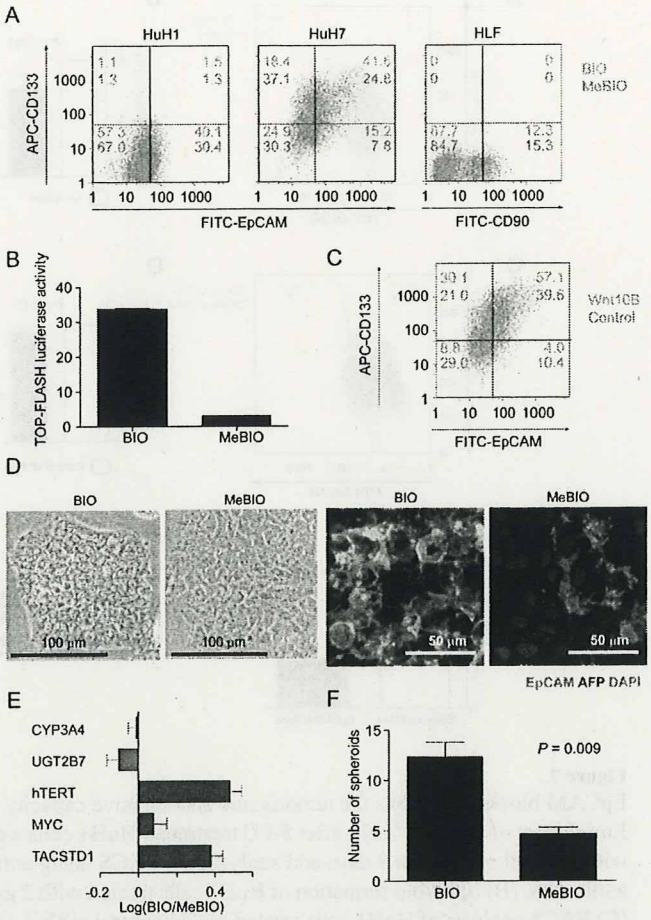

Figure 6.

Wnt/β-catenin signaling augments EpCAM$^+$ HCC cells. (A) Flow cytometer analysis of HuH1, HuH7, and HLF cells treated with 2μM of BIO (orange) or MeBIO (green) for 10 days and stained with anti-EpCAM, anti-CD133 and anti-CD90 antibodies. (B) TOP-FLASH luciferase assays of HuH7 cells treated with 2μM of BIO (red) or MeBIO (green). (C) Flow cytometer analysis of HuH7 cells cultured in the normal media (DMEM supplemented with 10% FBS) or Wnt10B conditioned media (details are described in the Materials and Methods). Cells were cultured in each medium for 2 weeks. (D) Representative phase contrast images (left panel, scale bar = 100 μm) or IF images (right panel, scale bar = 50 μm) of HuH7 cells treated with 2μM of BIO or MeBIO for 14 days. (E) qRT-PCR analysis of representative HpSC-HCC related genes in HuH7 cells treated with 2μM of BIO or MeBIO for 14 days. (F) Spheroid formation assay of HuH7 cells treated with 2μM of BIO or MeBIO for 14 days (mean ± SD).

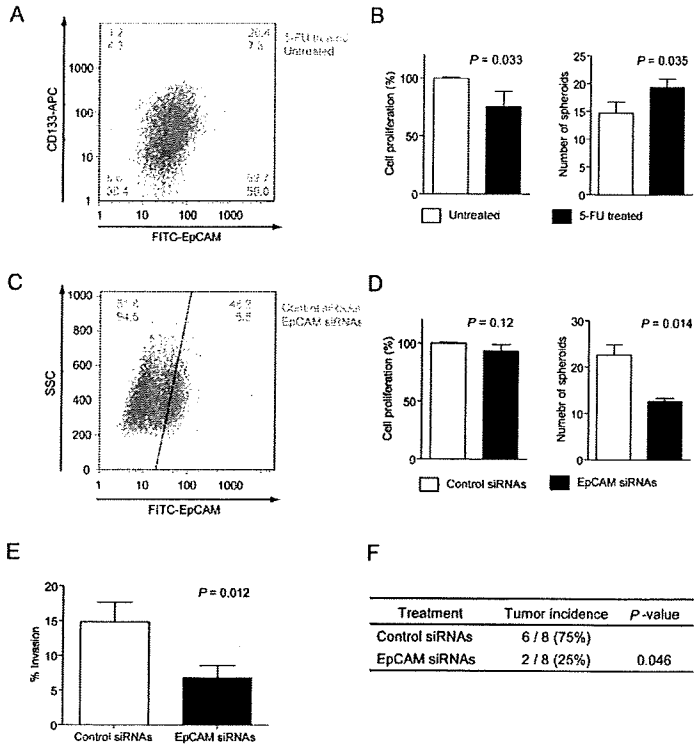

F

Treatment	Tumor incidence	*P*-value
Control siRNAs	6 / 8 (75%)	
EpCAM siRNAs	2 / 8 (25%)	0.046

Figure 7.

EpCAM blockage inhibits the tumorigenic and invasive capacity of EpCAM$^+$ HCC cells. (A) Enrichment of EpCAM$^+$ cells after 5-FU treatment. HuH1 cells were without (green) or treated with 2 μg/ml of 5FU for 3 days and analyzed by FACS using anti-EpCAM and anti-CD133 antibodies. (B) Spheroid formation of HuH1 cells treated with 2 μg/ml of 5FU (red) for 3 days. (C) FACS analysis of HuH1 cells treated with a control siRNA (orange) or EpCAM-specific siRNA (green) at day 3 after transfection. Spheroid formation (D) or invasive capacity (E) of EpCAM$^+$ HuH1 cells transfected with a control siRNA or EpCAM-specific siRNA. Experiments were performed in triplicate and the data are shown as mean ± SD. (F) Inhibition of tumor formation *in vivo* by EpCAM gene silencing. EpCAM$^+$ HuH1 cells were transfected with siRNA oligos and 1,000 cells were injected 24 hours after transfection.

Table 1

The tumor-initiating capacity of $EpCAM^+$ cells from clinical HCC specimens.

HCC Patients			No. of cells injected	Tumor incidence (mice with tumors/total # of mice injected)	
No.	% of $EpCAM^+$ HCC cells	Groups		2 months	3 months
1	5.2	$EpCAM^{\pm}$	1×10^3	0/3	0/3
			1×10^4	2/3	2/3
			1×10^5	2/2	2/2
		$EpCAM^-$	1×10^5	0/3	0/3
			1×10^6	0/2	0/2
2	1.4	$EpCAM^{\pm}$	1×10^3	0/2	0/2
			1×10^4	0/1	1/1
		$EpCAM^-$	1×10^4	0/3	0/3
			1×10^5	0/2	0/2

Developmental Biology 337 (2010) 405–414

Contents lists available at ScienceDirect

Developmental Biology

journal homepage: www.elsevier.com/developmentalbiology

Cv2, functioning as a pro-BMP factor via twisted gastrulation, is required for early development of nephron precursors

Makoto Ikeya [a,*,1], Kumi Fukushima [a], Masako Kawada [a], Sachiko Onishi [b], Yasuhide Furuta [c], Shigenobu Yonemura [b], Toshio Kitamura [d], Tetsuya Nosaka [e], Yoshiki Sasai [a,*]

[a] Organogenesis and Neurogenesis Group, RIKEN Center for Developmental Biology, 2-2-3 Minatojima-minamimachi, Chuo, Kobe 650-0047, Japan
[b] Electron Microscope Laboratory, RIKEN Center for Developmental Biology, Kobe 650-0047, Japan
[c] Department of Biochemistry and Molecular Biology, M.D. Anderson Cancer Center, University of Texas, Houston, TX 77030, USA
[d] Division of Cellular Therapy, The Institute of Medical Science, University of Tokyo, Tokyo 108-8639, Japan
[e] Department of Microbiology, Mie University Graduate School of Medicine, Tsu, Mie 514-8507, Japan

ARTICLE INFO

Article history:
Received for publication 8 July 2009
Revised 8 November 2009
Accepted 9 November 2009
Available online 13 November 2009

Keywords:
BMP
Kidney
Organogenesis
Genetic interactions

ABSTRACT

The fine-tuning of BMP signals is critical for many aspects of complex organogenesis. In this report, we show that the augmentation of BMP signaling by a BMP-binding secreted factor, Crossveinless2 (Cv2), is essential for the early embryonic development of mammalian nephrons. In the *Cv2*-null mouse, the number of cap condensates (clusters of nephron progenitors, which normally express Cv2) was decreased, and the condensate cells exhibited a reduced level of aggregation. In these $Cv2^{-/-}$ condensates, the level of phosphorylated Smad1 (pSmad1) was substantially lowered. The loss of a *Bmp7* allele in the $Cv2^{-/-}$ mouse enhanced the cap condensate defects and further decreased the level of pSmad1 in this tissue. These observations indicated that Cv2 has a pro-BMP function in early nephrogenesis. Interestingly, the renal defects of the $Cv2^{-/-}$ mutant were totally suppressed by a null mutation of *Twisted gastrulation* (*Tsg*), which encodes another BMP-binding factor, showing that Cv2 exerts its pro-BMP nephrogenic function Tsg-dependently. By using an embryonic kidney cell line, we presented experimental evidence showing that Cv2 enhances pro-BMP activity of Tsg. These findings revealed the molecular hierarchy between extracellular modifiers that orchestrate local BMP signal peaks in the organogenetic microenvironment.

Introduction

In terrestrial amniotes, the kidney is an indispensable and complex organ that maintains fluid homeostasis and blood pressure. Its anlage is a tissue called the metanephros. In the mouse, metanephric development starts about embryonic day (E) 10.5 with the demarcation of the metanephric blastema in the caudal part of the intermediate mesoderm, followed by reciprocal inductions between the blastema and the Wolffian duct (Vainio and Lin, 2002). In response to metanephric blastema-derived signals, the ureteric bud forms from the Wolffian duct, invades the metanephric blastema, and successively branches to form the collecting ducts. Conversely, ureteric bud-derived signals induce the formation of metanephric blastema-derived condensates (cap condensates) around the tips of collecting ducts; the cells forming the condensates will ultimately give rise to the nephrons, which carry out the functions of the adult kidney (Kobayashi et al., 2008). Although the signaling networks that regulate duct branching have been extensively studied (Shah et al., 2004), relatively little is known about the molecular mechanism of how cap condensates are formed and maintained (Kobayashi et al., 2008; Oxburgh et al., 2004).

The Bone Morphogenetic Protein (BMP) family is a class of secreted signaling proteins that belong to the transforming growth factor-beta (TGFβ) superfamily; they have diverse effects on the control of embryogenesis, including kidney development (Cain et al., 2008; Godin et al., 1998; Hogan, 1996; Simic and Vukicevic, 2005). An intriguing feature of BMP signaling is the presence of various extracellular BMP inhibitors (i.e., anti-BMP factors), such as Chordin, Noggin, Follistatin, Cerberus, and Gremlin (Glinka et al., 1997; Hemmati-Brivanlou et al., 1994; Hsu et al., 1998; Lamb et al., 1993; Sasai et al., 1995, 1994; Smith and Harland, 1992). Moreover, recent studies show that there are some proteins that bind to BMPs extracellularly and augment their signaling (i.e., pro-BMP factors). One protein with pro-BMP functions is Crossveinless2 (Cv2; also called Bmper), which enhances BMP signaling during wing cross-vein formation in *Drosophila*, as well as in neural crest emigration in the chick embryo, dorsal-ventral patterning of the zebrafish gastrula, and some cultured cell lines (Coles et al., 2004; Conley et al., 2000; Kamimura et al., 2004; Kelley et al., 2009; Moser et al., 2007; Rentzsch et al., 2006; Serpe et al., 2008).

* Corresponding authors. Fax: +81 78 306 1854.
E-mail addresses: mikeya@cdb.riken.jp (M. Ikeya), yoshikisasai@cdb.riken.jp (Y. Sasai).
[1] Present address: Department of Cell Modulation, Institute of Molecular Embryology and Genetics, Kumamoto University, Honjo 2-2-1, Kumamoto 860-0811, Japan.

0012-1606/$ – see front matter © 2009 Elsevier Inc. All rights reserved.
doi:10.1016/j.ydbio.2009.11.013